Journal of ELECTRONIC MATERIALS, Vol. 39, No. 12, 2010
DOI: 10.1007/s11664-010-1381-3

A New Nonlinear Optically Active Donor–Acceptor-Type Conjugated Polymer: Synthesis and Electrochemical and Optical Characterization

M.G. MANJUNATHA,[1] A.V. ADHIKARI,[1,3] P.K. HEGDE,[1] C.S. SUCHAND SANDEEP,[2] and REJI PHILIP[2]

1.—Organic Chemistry Division, Department of Chemistry, National Institute of Technology Karnataka, Surathkal, Mangalore 575025, India , 2.—Light and Matter Physics Group, Raman Research Institute, C.V. Raman Avenue, Sadashivanagar, Bangalore 560080, India. 3.—e-mail: avchem@nitk.ac.in; avadhikari123@yahoo.co.in

A new donor–acceptor-type poly[3-{5-[3,4-didodecyloxy-5-(1,3,4-oxadiazol-2-yl)thiophen-2-yl]-1,3,4-oxadiazol-2-yl}-9-dodecyl-9*H*-carbazole] (**P**) has been synthesized through multistep reactions. The new polymer **P** exhibited good thermal stability and film-forming behavior. The electrochemical band gap is estimated to be 2.15 eV. The polymer emits intense green fluorescence in the solid state. Third-order nonlinear optical (NLO) studies showed that the strong absorptive nonlinearity observed for the polymer is of the optical limiting type, which is due to an "effective" three-photon absorption (3PA) process. This 3PA process can have potential applications in photonic devices. The studies revealed that the new polymer **P** is a promising material for development of efficient optoelectronic devices.

Key words: Donor–acceptor conjugated polymer, *N*-dodecyl carbazole, 1,3,4-oxadiazole, electrochemical properties, fluorescence, 3PA, optical limiting

INTRODUCTION

During the last decade, the search for new nonlinear optical (NLO) materials has intensified because of their potential applications in integrated optics such as in optical modulation, optical communications, optical data storage, and optical power limiting.[1–4] Amongst various materials, organic compounds have turned out to be attractive, mainly due to their versatility, high nonlinearity, and the flexibility in tuning their optical properties. Recently, conjugated polymeric systems have emerged as a promising class of NLO materials, characterized by large third-order susceptibility along the polymer chain directions. These macromolecules offer good flexibility at both molecular and bulk levels, so that structural modifications necessary to optimize them for specific device applications are possible. Since the nonlinear response of these systems is determined primarily by their chemical structure, one can design unique molecular structures and synthesize compounds with enhanced nonlinear response by introducing suitable substituent groups.

Among various conjugated polymers, the third-order optical nonlinearity of thiophene-based conjugated polymers is currently under investigation, mainly because of their chemical stability, easy processability, and readiness of functionalization.[5–7] Good film-forming behavior, solubility, and adequate mechanical properties have made them better choices for device fabrication in comparison with their inorganic counterparts. For example, nonlinear optical properties can be synthetically tuned in polythiophenes by introducing electron-releasing and electron-accepting segments in the polymer chain which would result in increased delocalization in the molecule. Following a similar strategy, Adhikari and coworkers have synthesized a few donor–acceptor-type polythiophenes and studied

(Received September 28, 2009; accepted September 3, 2010; published online September 30, 2010)

the relationship between their structure and NLO properties.[8] It was found that electron-releasing and electron-accepting groups along the polymer backbone would be a promising molecular design for enhancing the third-order NLO properties.

Apart from NLO, conjugated polymers find applications in optoelectronic devices such as light-emitting diodes (LEDs), field-effect transistors, electrochemical cells, and organic photovoltaic cells. The newly developed polymers, poly(1,4-phenylenevinylene) (PPV),[9] poly(*p*-phenylene) (PPs),[10] polyfluorenes (PFs),[11] and polythiophenes (PTs),[12] have been the focus of such investigations recently.

Based on these facts, designs for synthesis of a new donor–acceptor-type conjugated poly(3,4-dialkoxy thiophene) with both electron and hole transport architecture have been considered. In recent years, carbazole-based polymers have attracted increasing interest because of their unique optical properties and strong hole-transporting ability in optoelectronic devices.[13] Therefore, in this context, it has been planned to incorporate the *N*-dodecylcarbazole moiety between 3,4-dialkoxy-substituted thiophenyl oxadiazole systems in our synthetic design to enhance electron donation within the polymer chain, with the expectation that the resulting molecule would exhibit better NLO properties. Furthermore, it has been predicted that the presence of the *N*-dodecylcarbazole moiety would influence the optical and electrochemical properties. Herein, we report the synthesis of a hitherto-unknown donor–acceptor-type conjugated polymer carrying the 3-{5-[3,4-didodecyloxy-5-(1,3,4-oxadiazol-2-yl)thiophen-2-yl]-1,3,4-oxadiazol-2-yl}-9-dodecyl-9*H*-carbazole unit and the investigation of its electrochemical and optical properties in detail. Furthermore, we report third-order NLO studies by the *Z*-scan method.

EXPERIMENTAL PROCEDURES

Materials

3,4-Didodecyloxythiophene-2,5-dicarbohydazide (**6**) was synthesized according to the reported procedure.[14] Dimethylformamide (DMF) and acetonitrile were dried over CaH_2. Thiodiglycolic acid, diethyl oxalate, 9*H*-carbazole, sodium hydride, *N*,*N*-dimethylcarbamoyl chloride, tetrabutylammonium perchlorate (TBAPC), and *n*-bromododecane were purchased from Lanchaster (UK) and used as received. All solvents and reagents were of analytical grade. They were purchased commercially and used without further purification.

Instrumentation

Infrared spectra of all intermediate compounds and polymers were recorded on a Nicolet Avatar 5700 Fourier-transform infrared (FT-IR) spectrometer (Thermo Electron Corporation). Ultraviolet–visible (UV–Vis) and fluorescence emission spectra were measured using GBC Cintra 101 UV–Vis and Perkin-Elmer LS55 spectrophotometers, respectively. ^{1}H nuclear magnetic resonance (NMR) spectra were obtained by using an AMX 400-MHz FT-NMR spectrophotometer using tetramethylsilane (TMS)/solvent signal as an internal reference. Mass spectra were recorded on a Jeol SX-102 (FAB) mass spectrometer. Elemental analyses were performed using a Flash EA1112 CHNS analyzer (Thermo Electron Corporation). The thermal stability of the polymer was analyzed by SII EXSTAR6000-TG/DTA6300 thermogravimetric analyzer (TGA). The molecular weight of the polymer was determined by gel permeation chromatography (GPC; Waters) using polystyrene standards in tetrahydrofuran (THF) solvent.

Cyclic Voltammetry

Cyclic voltammetry (CV) was employed to determine redox potentials of the new polymer and then to estimate the highest occupied molecular orbital (HOMO) and the lowest unoccupied molecular orbital (LUMO) energy of the polymer, which are of importance to determine the band gap. The cyclic voltammogram of the polymer coated on a glassy carbon electrode was measured using an AUTOLAB PGSTAT 30 electrochemical analyzer, using a Pt counterelectrode and a Ag/AgCl reference electrode, immersed in the electrolyte [0.1 M $(n\text{-Bu})_4NClO_4$ in acetonitrile] at a scan rate of 25 mV s^{-1}.

Z-Scan Measurement

The *Z*-scan technique, which was developed by Sheik-Bahae et al.,[14] is now widely used for measuring the nonlinear absorption coefficient and the nonlinear refractive index of the materials. A variation of the method called "open-aperture *Z*-scan" gives information about the nonlinear absorption coefficient. Here, a Gaussian laser beam is used for exciting the sample, and its propagation direction is taken as the *z*-axis. The beam is focused using a convex lens, and the focal point is taken as $z = 0$. The maximum energy density of the beam is at its focus, which will symmetrically reduce towards either side of it, for positive and negative values of *z*. In the experiment (Fig. 1) the sample is placed in the beam at different positions with respect to the focus (different values of *z*), and the corresponding transmissions are measured. The sample sees a different laser intensity at each position, *z*. If the intensity corresponding to each *z* is known, then the position-dependent transmission can be easily converted to intensity-dependent transmission. From this nonlinear transmission information the nonlinear absorption coefficient can be calculated.

We used a stepper-motor-controlled linear translation stage in our setup to move the sample through the beam in precise steps. The sample was taken in a 1-mm cuvette. The transmission of the sample at each point was measured by means of two pyroelectric energy probes (Rj7620; Laser Probe

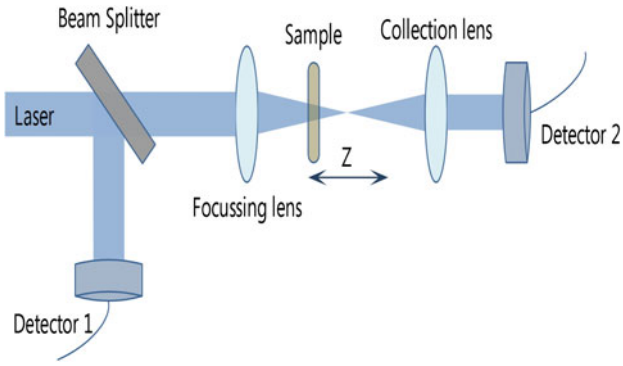

Fig. 1. Schematic diagram of the open-aperture *Z*-scan setup.

Inc.). One energy probe monitored the input energy, while the other monitored the energy transmitted through the sample. The second harmonic output (532 nm) of a Q-switched Nd:YAG laser (Minilite; Continuum Inc.) was used for exciting the molecules. The temporal width (full-width at half-maximum, FWHM) of the laser pulses was 5 ns. A pulse energy of 180 μJ was used for the experiments. The pulses were fired in the "single-shot" mode, allowing sufficient time between successive pulses to avoid accumulative thermal effects in the sample.

Synthesis of *N*-Dodecylcarbazole (2)

To a mixture of 0.1 mol carbazole dissolved in DMF was added 0.2 mol sodium hydride (NaH). The mixture was refluxed for 0.5 h and then 0.1 mol 1-bromo dodecane was added dropwise. The mixture was refluxed for 6 h. After cooling to room temperature, the mixture was poured into water (200 mL), and the organic layer was extracted with methylene dichloride three times (50 mL each). It was then dried with anhydrous magnesium sulfate. Finally the solvent was removed by rotary evaporation to obtain a thick liquid. Yield: 85%. ^{1}H NMR (400 MHz, $CDCl_3$) shifts δ (ppm): 2H (m, Aromatic), 8.14–8.12; 4H (m, Aromatic), 7.50–7.42; 2H (m, Aromatic), 7.25–7.23; 2H (t, -NCH_2-), 4.20; 2H (m, -NCH_2CH_2-), 1.90–1.87; 18H (m, -$(CH_2)_9$-), 1.43–1.26; 3H (t, -CH_3), 0.90. FT-IR (KBr, cm^{-1}): -C-H stretch, 2969 and 2935. Element. Anal. Calcd. For $C_{25}H_{33}N$: C, 85.91; H, 9.91; N, 4.17. Found: C, 85.62; H, 10.06; N, 4.12.

Synthesis of 3,6-Bis(*N*,*N*-dimethylcarbamoyl)-9-dodecylcarbazole (3)

To a well-stirred mixture of 0.04 mol aluminum chloride and 30 mL ethylene chloride under nitrogen atmosphere was added a clear solution of 0.02 mol *N*-dodecylcarbazole (**13**) in 30 mL ethylene chloride. A solution of 0.04 mol *N*,*N*-dimethylcarbamoyl chloride in 30 mL ethylene chloride was added dropwise over 30 min. The mixture was refluxed for 24 h under nitrogen atmosphere. Then, the reaction mixture was cooled to room temperature and poured into 100 mL of water and extracted with chloroform three times (30 mL each). The combined organic layer was washed with water until the washings were neutral to litmus paper and dried over anhydrous magnesium sulfate. The solvent was evaporated under reduced pressure, and the residue was purified by silica gel column chromatography using ethyl acetate/hexane (7:3) as eluent. Yield: 60%. ^{1}H NMR (400 MHz, $CDCl_3$) shifts δ (ppm): 2H (m, Aromatic), 8.15–8.10; 2H (m, Aromatic), 7.60–7.49; 2H (m, Aromatic), 7.32–7.29; 2H (t, -NCH_2-), 4.18; 12H (s, -$N(CH_3)_2$), 3.15; 2H (m, -NCH_2CH_2-), 1.92–1.88; 18H (m, -$(CH_2)_9$-), 1.40–1.24; 3H (t, -CH_3), 0.92. FT-IR (KBr, cm^{-1}): -C-H stretch, 2972 and 2939; >C=O stretch, 1685. Element. Anal. Calcd. For $C_{30}H_{43}N_3O_2$: C, 75.43; H, 9.07; N, 8.80. Found: C, 75.62; H, 9.18; N, 8.68.

Synthesis of *N*-Dodecylcarbazole-3,6-dicarboxylic Acid (4)

A mixture of 0.01 mol compound **3** and 50 mL 20% ethanolic potassium hydroxide was heated under reflux for 6 h. The solvent was evaporated, and the residue was poured onto an excess of water, then the solution was filtered and acidified using concentrated HCl. The precipitate was collected by filtration and washed with water. The crude product was recrystallized using ethanol to give a white solid. Yield: 80%. M.p.: >250°C. FAB HRMS: *m/z*, 424. ^{1}H NMR (400 MHz, $CDCl_3$) shifts δ (ppm): 2H (s, -COOH), 12.52; 2H (m, Aromatic), 8.18–8.12; 2H (m, Aromatic), 7.62–7.52; 2H (m, Aromatic), 7.35–7.32; 2H (t, -NCH_2-), 4.22; 2H (m, -NCH_2CH_2-), 1.94–1.89; 18H (m, -$(CH_2)_9$-), 1.42–1.22; 3H (t, -CH_3), 0.94. FT-IR (KBr, cm^{-1}): -O-H stretch, 3450; -C-H stretch, 2975 and 2942; >C=O stretch,1680. Element. Anal. Calcd. For $C_{26}H_{33}NO_4$: C, 73.73; H, 7.85; N, 3.31. Found: C, 73.48; H, 7.98; N, 3.38.

Synthesis of *N*-Dodecylcarbazole-3,6-dicarbonyl Chloride (5)

A mixture of carbazole diacid **4** and 15 mL thionyl chloride was refluxed for 8 h. The excess thionyl chloride was removed by distillation. The residue was purified by recrystallization from dichloromethane to afford a light yellow powder. Yield: 75%. ^{1}H NMR (400 MHz, $CDCl_3$) shifts δ (ppm): 2H (m, Aromatic), 8.12–8.07; 2H (m, Aromatic), 7.60–7.53; 2H (m, Aromatic), 7.32–7.27; 2 h (t, -NCH_2-), 4.21; 2H (m, -NCH_2CH_2-), 1.92–1.87; 18H (m, -$(CH_2)_9$-), 1.35–1.20; 3H (t, -CH_3), 0.91. FT-IR (KBr, cm^{-1}): -C-H stretch, 2979 and 2940; >C=O stretch, 1690. Element. Anal. Calcd. For $C_{26}H_{31}Cl_2NO_2$: C, 67.82; H, 6.79; N, 3.04. Found: C, 67.48; H, 6.94; N, 3.18.

Synthesis of 3,4-Didodecyloxythiophene-2,5-carboxydihydrazide (6)

3,4-Didodecyloxythiophene-2,5-dicarbohydazide (**6**) was synthesized according to the reported procedure.[15]

The structure of the compound was confirmed by different spectroscopic techniques. Yield: 85%. ^{1}H NMR (400 MHz, $CDCl_3$) shifts δ (ppm): 2H (s, > N-H), 8.33; 4H (s, -NCH_2), 4.90; 4H (t, -OCH_2-), 4.15; 40H (m, -$(CH_2)_{10}$-), 1.27–1.81; 6H (t, -CH_3), 0.88. FT-IR (KBr, cm^{-1}): >N-H stretch, 3284; -C-H stretch, 2966 and 2931; >C=O stretch, 1610. Anal. Calcd. for $C_{30}H_{56}N_4O_4S$: C, 63.34; H, 9.92; N, 9.85; S, 5.64. Found: C, 62.60; H, 10.40; N, 9.06; S, 5.12.

Synthesis of Precursor Polyhydrazide (PH)

To a mixture of 1 equiv. dihydrazide (**6**), 2 equiv. anhydrous aluminum chloride, and 0.1 mL pyridine, 1 equiv. carbazole diacid chloride (**5**) was added slowly at room temperature with stirring, and stirring was continued for 5 h. Furthermore, it was heated at 80°C for 20 h. After cooling to room temperature the reaction mixture was poured into ice-cold water, and the precipitate separated was collected by filtration. It was washed with water followed by acetone and finally dried in vacuum to get the polyhydrazide **PH**. Yield: 80%. FT-IR (KBr, cm^{-1}): >N-H stretch, 3294; >C=O stretch, 1630. Anal. Calcd. for $C_{56}H_{85}N_5O_6S$: C, 70.33; H, 8.96; N, 7.32; S, 3.35. Found: C, 69.95; H, 8.56; N, 7.48; S, 3.15.

Synthesis of Polymer (P)

A mixture of polyhydrazide (0.5 g) and 20 mL phosphorus oxychloride was heated at 100°C for 8 h with stirring under nitrogen atmosphere. The reaction mixture was then cooled to room temperature and poured into excess ice-cold water. The resulting precipitate was collected by filtration, washed with water followed by acetone, and finally dried in a vacuum oven to get the polymer **P**. Yield: 75%. ^{1}H NMR (400 MHz, $CDCl_3$), shifts δ (ppm): 2H (m, Aromatic), 8.18–8.12; 2H (m, Aromatic), 7.55–7.49; 2H (m, Aromatic), 7.36–7.30; 4H (t, -OCH_2-), 4.32; 2H (t, -NCH_2-), 4.21; 60H (m, -$(CH_2)_{30}$-), 1.95–1.20; 9H (m, -CH_3), 0.95. FT-IR (KBr, cm^{-1}): C=N stretch, 1590. Anal. Calcd. for $C_{56}H_{81}N_5O_4S$: C, 73.08; H, 8.87; N, 7.61; S, 3.48. Found: C, 72.72; H, 8.56; N, 7.48; S, 3.23.

RESULTS AND DISCUSSION

Synthesis and Characterization of the Polymer

Scheme 1 shows the designed synthetic route for the preparation of monomer **5** and the polymer **P**. The required *N*-dodecylcarbazole (**2**) was synthesized by reaction of *n*-bromododecane with carbazole (**1**) in presence of NaH. This *N*-dodecylcarbazole (**2**) was converted into 3,6-bis(*N*,*N*-dimethylcarbamoyl)-9-dodecylcarbazole (**3**) by the action of *N*,*N*-dimethylcarbamoyl chloride in the presence of anhydrous aluminum chloride ($AlCl_3$), which on hydrolysis in alcoholic KOH afforded *N*-dodecylcarbazole-3,6-dicarboxylic acid (**4**). Then, compound **4** was treated with excess thionyl chloride to yield *N*-dodecylcarbazole-3,6-dicarbonyl

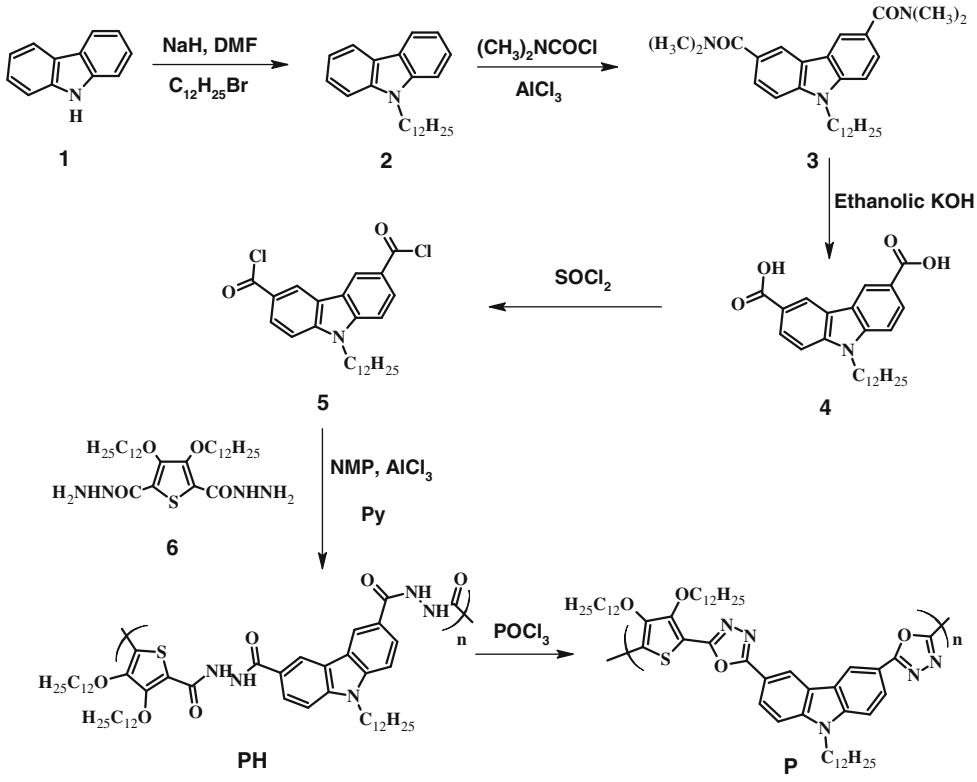

Scheme 1. Designed synthetic route for preparation of polymer **P**.

chloride (**5**). Formation of 3,4-didodecyloxythiophene-2,5-carboxydihydrazide (**6**) from the corresponding diester was evidenced by its FT-IR and ^{1}H NMR spectral data. Its FT-IR spectrum showed sharp peaks at 3284 cm^{-1} and 1610 cm^{-1}, indicating the presence of -NH_2 and >C=O groups, respectively. Its ^{1}H NMR spectrum displayed peaks at δ of 8.33 ppm (s, 2H) and 4.90 ppm (s, 4H) for >NH and -NH_2 protons, respectively. The precursor polyhydrazide **PH** was prepared by polycondensation of **5** with **6** in the presence of anhydrous aluminum chloride and pyridine. The polyhydrazide was converted into target polymer **P** through cyclodehydration reaction using phosphorus oxychloride as the dehydrating agent. The structures of the newly synthesized compounds were confirmed by FT-IR, ^{1}H NMR, mass spectral, and elemental analyses.

The formation of *N*-dodecylcarbazole (**2**) from carbazole (**1**) was evidenced by its ^{1}H NMR spectral data. Its ^{1}H NMR spectrum displayed multiple peaks at δ of 4.2 ppm and 0.9 ppm to 1.9 ppm, corresponding to alkyl chain protons. Conversion of *N*-dodecylcarbazole (**2**) to 3,6-bis(*N*,*N*-dimethylcarbamoyl)-9-dodecylcarbazole (**3**) was confirmed by its FT-IR and ^{1}H NMR. Its FT-IR spectrum exhibited a sharp peak at 1685 cm^{-1} for >C=O group, and its ^{1}H NMR spectrum showed -$N(CH_3)_2$ protons as a singlet at δ value of 3.15 ppm. Hydrolysis of compound **3** to carbazole diacid **4** was established by its FT-IR, ^{1}H NMR, and mass spectral data. Its FT-IR spectrum showed a broad absorption peak due to -OH groups. Furthermore, in its ^{1}H NMR spectrum (Fig. 2), peaks corresponding to -$N(CH_3)_2$ protons disappeared and the acid protons resonated at δ value of 12.52 ppm. The mass spectrum of **4** showed molecular ion peak at m/z = 424, which corresponds to its molecular formula $C_{26}H_{33}NO_4$. The structure of *N*-dodecylcarbazole-3,6-dicarbonyl chloride (**5**) was determined based on FT-IR and ^{1}H NMR spectral analyses. Its FT-IR and ^{1}H NMR spectra did not show peaks corresponding to protons of -COOH groups.

The chemical structure of precursor polyhydrazide **PH** was evidenced by its FT-IR spectral and elemental analyses. The FT-IR spectrum (Fig. 3) of **PH** exhibited sharp peaks at 3294 cm^{-1} and 1630 cm^{-1}, corresponding to >N-H and >C=O groups, respectively. Successful conversion of polyhydrazide **PH** into polyoxadiazole **P** was confirmed by its FT-IR spectrum. In its FT-IR spectrum (Fig. 4), the disappearance of >C=O and >N-H stretching absorption bands and the appearance of a sharp peak at around 1590 cm^{-1} due to imine of the oxadiazole ring indicate the cyclization. The chemical structure of the polymer was confirmed by FT-IR, ^{1}H NMR spectroscopy, and elemental analysis. The FT-IR spectrum of **P** showed characteristic absorption peaks at 2920 cm^{-1}, 2848 cm^{-1} (C-H stretching aliphatic segments), 1590 cm^{-1} (1,3,4-oxadiazole), 1468 cm^{-1} (aromatic), and 1062 cm^{-1} (=C-O-C= stretching of oxadiazole). The ^{1}H NMR spectra of polymer **P** showed a multiplet at δ of 7.30 ppm to 8.18 ppm due to aromatic protons (carbazole ring). Peaks corresponding to the protons of the alkoxy (-OCH_2-) groups at 3- and 4-positions of the thiophene ring and -NCH_2- protons of *N*-alkyl chain appeared at δ values of 4.32 ppm and 4.21 ppm, respectively. Complex multiple peaks at δ values ranging from 0.95 ppm to 1.95 ppm were observed due to remaining protons of *N*- and *O*-alkyl chains. The elemental analysis result of the polymer was in agreement with its expected empirical formula. The weight-average molecular weight of the polymer (THF-soluble part) was found to be 6870. Thermogravimetric analysis (TGA) of the polymer was carried out under nitrogen atmosphere at a heating rate of 5°C min^{-1}. As shown in Fig. 5, polymer **P** was thermally stable up to 300°C.

Electrochemical Properties

The electrochemical study of the polymer **P** was carried out using an AUTOLAB PGSTAT30 electrochemical analyzer, and the corresponding electrochemical data are summarized in Table I.

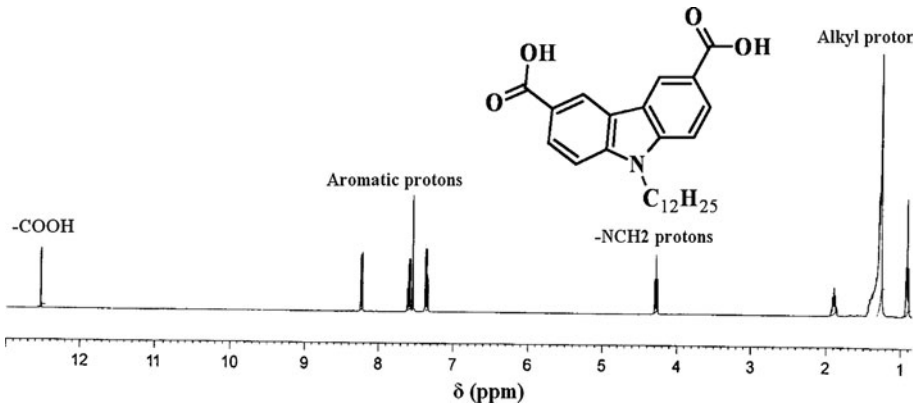

Fig. 2. ^{1}H NMR spectrum of *N*-dodecylcarbazole-3,6-dicarboxylic acid (**4**).

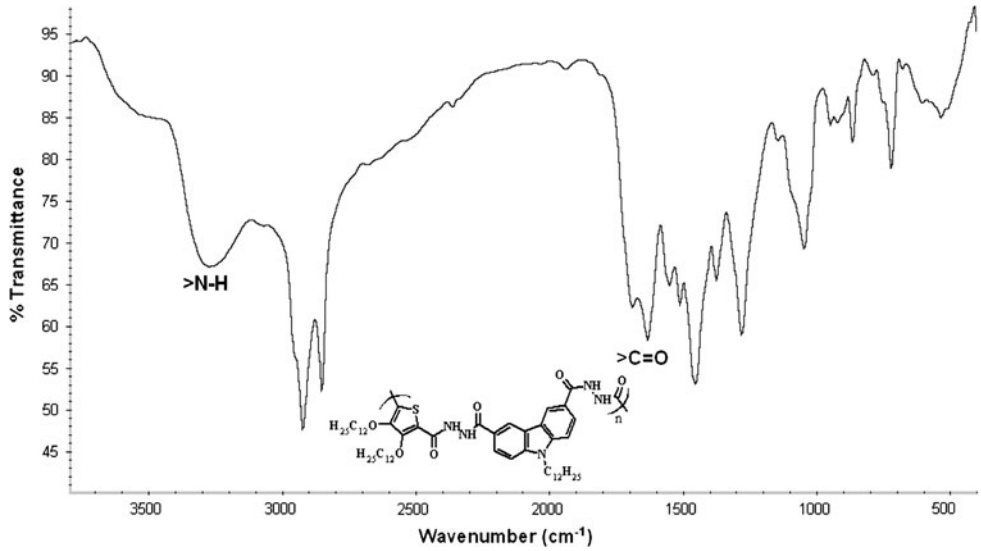

Fig. 3. FT-IR spectrum of polyhydrazide **PH**.

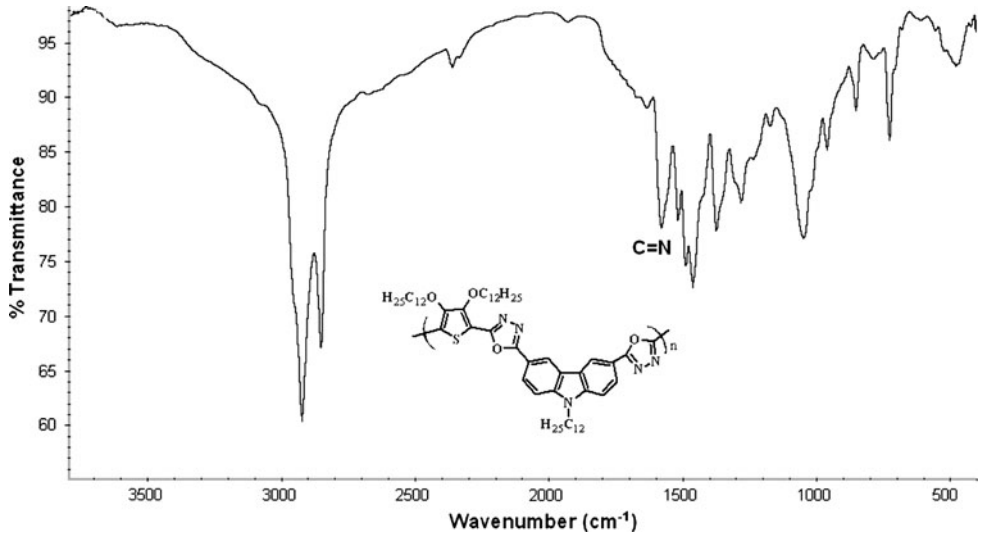

Fig. 4. FT-IR spectrum of polymer **P**.

While sweeping cathodically (Fig. 6), polymer **P** showed a reduction peak at −1.25 V. This reduction potential is lower than that of 2-(4-biphenyl)-5-(4-*tert*butylphenyl)-1,3,4-oxadiazole (PBD),[16,17] one of the most widely used electron-transporting materials. In the anodic sweep (Fig. 7), the polymer showed an oxidation peak at 1.70 V. The onset potentials of *n*- and *p*-doping processes can be used to estimate the HOMO and LUMO of the polymer. As reported in the literature,[18–20] $E_{HOMO} = -[E^{oxd}_{onset} + 4.4\,eV]$ and $E_{LUMO} = -[E^{red}_{onset} - 4.4\,eV]$, where E^{oxd}_{onset} and E^{red}_{oxd} are the onset potentials versus standard calomel electrode (SCE) for the oxidation and reduction of the polymer.

According to the above equations, the HOMO energy level of the polymer was estimated to be −5.74 eV, which is comparable to that of CN-PPV. The LUMO energy level (−3.59 eV) is lower than that of PPV and some other reported conjugated *p*-type conjugated polymers, indicating that the polymer has better electron-transporting properties. The very high electron affinity of this polymer may be attributed to the incorporation of electron-deficient oxadiazole ring in the polymer backbone. From the onset potentials of oxidation and reduction processes, the band gap of the polymer is estimated to be 2.15 eV. It is clear from the results that the polymer has good charge-carrying properties, which is one of the major requirements for optoelectronic device applications.

Linear Optical Properties

The UV–Vis absorption and fluorescence emission spectra of the polymer **P** were recorded both in solution and in thin-film form. As shown in Fig. 8,

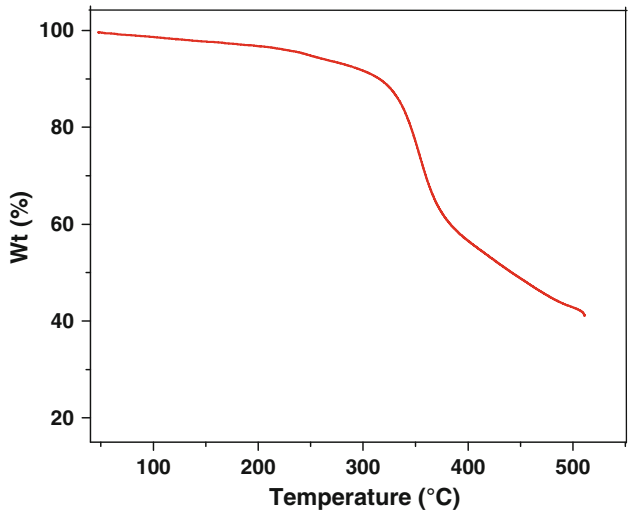

Fig. 5. TGA trace of the polymer.

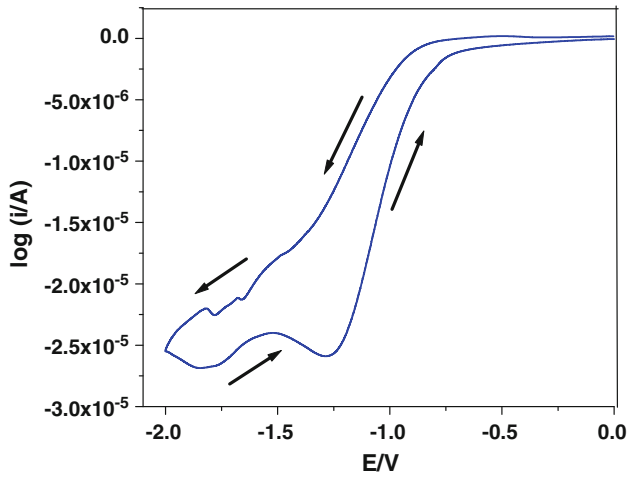

Fig. 6. Reduction cyclic voltammetric trace of the polymer.

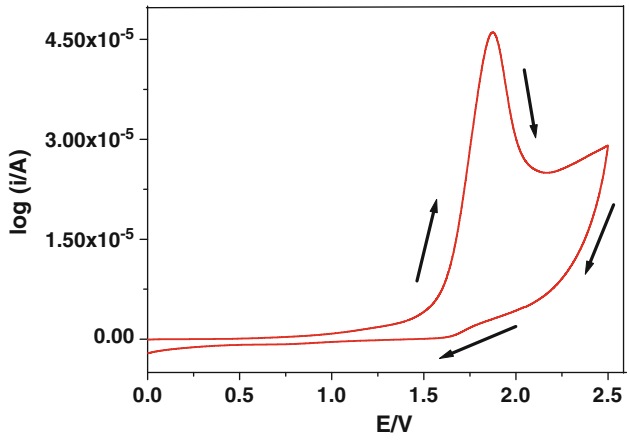

Fig. 7. Oxidation cyclic voltammetric trace of the polymer.

the absorption maximum of the polymer in dilute $CHCl_3$ solution was 385 nm. The absorption spectrum of the polymer in thin film (Fig. 8) showed a 23 nm bathochromic shift with respect to that obtained from its solution, indicating the presence of interchain interactions in the solid state. Its optical band gap (E_g) was calculated from the absorption edge of the spectrum and found to be 2.21 eV, quite close to that obtained by the electrochemical method (Table I).

As shown in Fig. 9, the emissive maximum (excitation wavelength 370 nm) of the polymer in dilute $CHCl_3$ solution was 484 nm. The fluorescence emission spectrum of the polymer in thin film (Fig. 9) showed a 23 nm redshift with respect to that obtained from its solution. The polymer emits intense green fluorescence in solid state with an emission peak of 507 nm. The Stokes shift was found to be 99 nm. The fluorescence quantum yield of the polymer in solution was determined to be 37% against quinine sulfate as a standard (10^{-5} M quinine sulfate in 0.1 M H_2SO_4). These results clearly indicate that the newly synthesized polymer **P** is a promising material for application in optoelectronic devices. Device fabrication and characterization are in progress.

Nonlinear Optical Properties

The linear absorption spectrum of polymer **P** showed that the excitation wavelength of 532 nm is close to one of the absorption edges. The linear absorption coefficient (α) for the polymer at 532 nm was 235.7 m^{-1}. As shown in Fig. 10, the polymer showed good optical limiting behavior, where the transmittance decreases when the pump fluence is increased. It is seen that a three-photon absorption

Table I. Molecular weight, electrochemical potential, and energy levels of the polymer

Polymer	M_n[a]	M_w[b]	PD[c]	E_{oxd}	E_{red}	E_{oxd} (Onset)	E_{red} (Onset)	E_{HOMO} (eV)	E_{LUMO} (eV)	E_g[d] (eV)
P	3120	6870	2.2	1.70	−1.25	1.40	−0.75	−5.74	−3.59	2.15

[a] Number-average molecular weight, [b] weight-average molecular weight, [c] polydispersity, [d]Electrochemical bandgap.

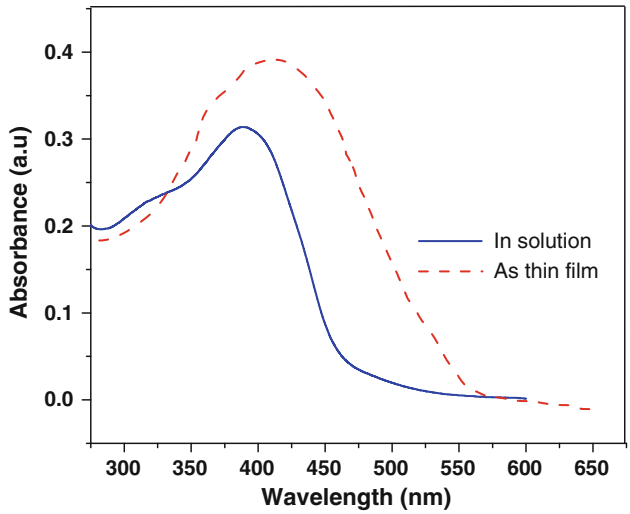

Fig. 8. UV–Vis absorption spectra of the polymer in solution and film form.

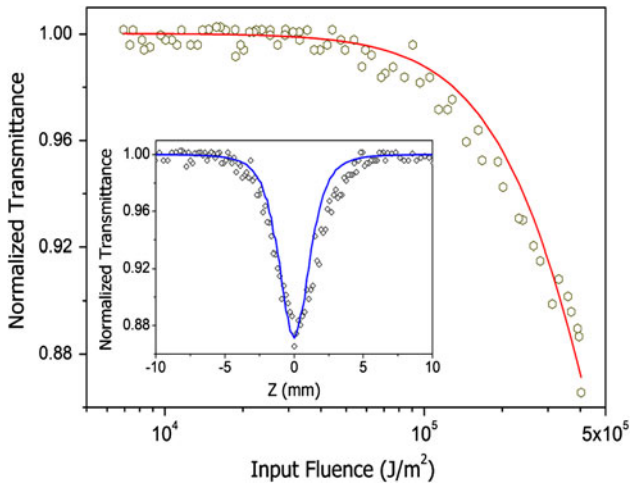

Fig. 10. Input fluence versus normalized transmittance for the polymer. *Inset* shows the *Z*-scan curve. *Hollow circles* show the data points and the *solid line* gives the best 3PA fit to the data.

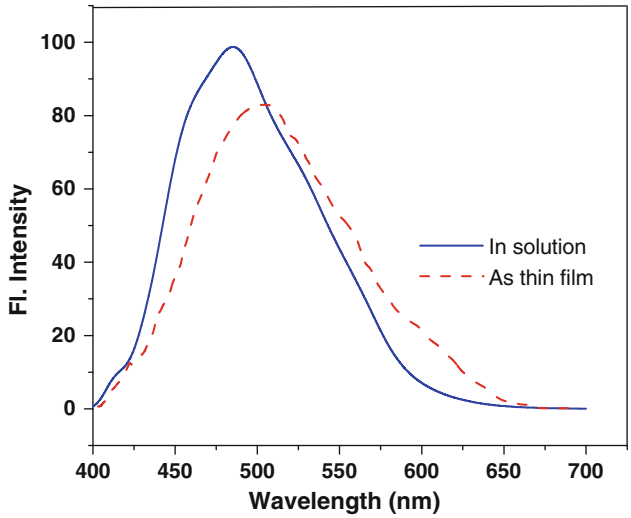

Fig. 9. Fluorescence emission spectra of polymer in solution and film form.

(3PA)-type process gives the best fit to the obtained experimental data. The *Z*-scan curves obtained were therefore numerically fitted to the nonlinear transmission equation for a three-photon absorption process, given by Eq. 1

$$T = \frac{(1-R)^2 \exp(-\alpha L)}{\sqrt{\pi} p_0} \times \int_{-\infty}^{+\infty} \ln\left[\sqrt{1+p_0^2 \exp(-2t^2)} + p_0 \exp(-t^2)\right] \mathrm{d}t, \quad (1)$$

where T is the transmission of the sample, R is the Fresnel reflection coefficient at the sample–air interface, α is the absorption coefficient, and L is the sample length. Here p_0 is given by $[2\gamma(1-R)^2 I_0^2 L_{\mathrm{eff}}]^{1/2}$, where γ is the three-photon absorption coefficient, and I_0 is the incident intensity. L_{eff} is given by $[1-\exp(-2\alpha L)]/2\alpha$. The value of the 3PA coefficient (γ) obtained from the curve fitting is 2.1×10^{-25} m^3 W^{-2}.

Considering the absorption spectra of the samples and recalling that pure three-photon absorption cross-sections are generally very low, it seems that the observed nonlinearity arises from sequential three-photon absorption involving excited states. Two-photon absorption followed by excited-state absorption is another possibility. Therefore the nonlinearity can be considered as an "effective" three-photon absorption process. In a pure 3PA process, three photons will be simultaneously absorbed and this is an instantaneous nonlinear optical phenomenon. Compared with the usual one-photon absorption process the cross-section for a 3PA is generally low, but it becomes significant when the samples are irradiated with intense laser pulses of picosecond or shorter duration. With nanosecond pulse excitation, accumulative nonlinear optical phenomena such as excited-state absorption and free carrier absorption become more prominent. Depending on the material system under study, excitation wavelength, and applied laser fluence, a combination of the instantaneous and accumulative nonlinear effects may take place. These, however, will appear like pure 2PA or pure 3PA in a simple transmission measurement such as the *Z*-scan. These combined nonlinearities can hence be termed "effective 2PA" and "effective 3PA" processes to distinguish them from pure 2PA and 3PA processes. Such absorptive nonlinearities involving real excited states have been reported earlier in C_{60} (fullerenes), semiconductors, metal

nanoclusters, fluorene derivatives, etc.[21–27] During the 3PA process, excitation is proportional to the cube of the incident intensity. This feature may help to obtain higher contrast and resolution in imaging, since 3PA provides stronger spatial confinement. With the availability of ultrafast pulsed lasers in recent years, significant progress in 3PA-based applications has been witnessed, including three-photon pumped lasing and 3PA-based optical limiting and stabilization.[28]

In π-conjugated polymeric systems, electrons can move in large molecular orbitals which result from linear superposition of the carbon p_z atomic orbitals, leading to very high optical nonlinearity, which increases with the conjugation length.[29] The polymer studied in the present work consists of thiophene ring substituted with dodecyloxy pendant at 3,4-position and *N*-dodecyl carbazole as electron-donating groups and 1,3,4-oxadiazole as an electron-withdrawing group. This leads to the formation of a donor–acceptor type of arrangement in the polymer backbone. The enhanced third-order nonlinearity in the polymer arises due to the high π-electron density along the polymeric chain, which is easily polarizable as a result of the alternating donor–acceptor arrangement.

CONCLUSIONS

A novel conjugated polymer **P** carrying 3-{5-[3,4-didodecyloxy-5-(1,3,4-oxadiazol-2-yl)thiophen-2-yl]-1,3,4-oxadiazol-2-yl}-9-dodecyl-9*H*-carbazole unit with donor and acceptor moieties in the molecular architecture has been successfully synthesized through multistep reactions. The newly synthesized monomers and the polymer were characterized using spectroscopic techniques. The polymer is found to be thermally stable up to 300°C. The electrochemical properties showed that the polymer possesses high-lying HOMO energy level (−5.74 eV) and low-lying LUMO energy level (−3.59 eV). This is attributed to the presence of alternating donor–acceptor conjugated units along the copolymer backbone. The linear optical properties revealed that the polymer has absorption maxima at 408 nm and emits intense green fluorescence in solid state. The nonlinear optical property of the polymer has been studied using the *Z*-scan technique. The polymer exhibited an "effective" three-photon absorption (3PA) behavior. The value of the three-photon absorption coefficient (γ) has been calculated. The absorptive nonlinearity observed is of the optical limiting type, which can have potential applications in photonic devices. The electrochemical and optical properties revealed that the polymer **P** is a new promising material for optoelectronic device applications.

ACKNOWLEDGEMENTS

The authors are grateful to CDRI, Lucknow, NMR Research Centre, IISc Bangalore, and RRL, Trivandrum, for providing instrumental analyses.

REFERENCES

1. R.L. Sutherland, *Handbook of Nonlinear Optics* (New York: Dekker, 1996).
2. J.W. Perry, K. Mansour, I.-Y.S. Lee, X.-L. Wu, P.V. Bedworth, C.-T. Chen, D. Ng, S.R. Marder, P. Miles, T. Wada, M. Tian, and H. Sasabe, *Science* 273, 1533 (1996).
3. P.N. Prasad and D.J. Williams, *Introduction to Nonlinear Optical Effects in Molecules and Polymers* (New York: Wiley, 1992).
4. A. Ronchi, T. Cassano, R. Tommasi, F. Babudri, A. Cardone, G.M. Farinola, and F. Naso, *Synth. Met.* 139, 831 (2003).
5. M. Nisoli, A. Cybo-Ottone, S. De Silvestri, V. Magni, R. Tubino, C. Botta, and A. Musco, *Phys. Rev. B* 147, 10881 (1993).
6. J. Roncali, *Chem. Rev.* 92, 711 (1992).
7. S. Kishino, Y. Ueno, K. Ochiai, M. Rikukawa, K. Sanui, T. Kobayashi, H. Kunugita, and K. Ema, *Phys. Rev. B* 58, R13430 (1998).
8. D. Udayakumar, A. John Kiran, A.V. Adhikari, K. Chandrasekharan, G. Umesh, and H.D. Shashikala, *Chem. Phys.* 331, 125 (2006).
9. J.H. Burroughes, D.D.C. Bradley, A.R. Brown, R.N. Marks, K. Mackay, R. Friend, P.L. Burn, and A.B. Holmes, *Nature* 347, 539 (1990).
10. G. Grem, G. Leditzky, B. Ullrich, and G. Leising, *Adv. Mater.* 4, 36 (1992).
11. M. Leclerc, *J. Polym. Sci. Part A: Polym. Chem.* 39, 2867 (2001).
12. J. Pei, W.-L. Yu, W. Haung, and A.J. Heeger, *Chem. Commun.* 1631, (2000).
13. H. Meng, Z.-K. Chen, W.-L. Yu, J. Pei, X.-L. Liu, Y.-H. Lai, and W. Huang, *Synth. Met.* 100, 297 (1999).
14. M. Sheik-Bahae, A.A. Said, T. Wei, D.J. Hagan, and E.W. Van Styrland, *IEEE J. Quantum Electron.* 26, 760 (1990).
15. P.K. Hegde, A.V. Adhikari, M.G. Manjunatha, C.S.S. Sandeep, and R. Philip, *Synth. Met.* 159, 1099 (2009).
16. M. Strukelj, F. Papadimitrakopoulos, T.M. Miller, and L.J. Rotheberg, *Science* 267, 1969 (1995).
17. S. Janietz and A. Wedel, *Adv. Mater.* 9, 403 (1997).
18. D.M. de Leeuw, M.M.J. Simenon, A.B. Brown, and R.E.F. Einerhand, *Synth. Met.* 87, 53 (1997).
19. A.K. Agrawal and S.A. Jenekhe, *Chem. Mater.* 8, 579 (1996).
20. C.-J. Yang and S.A. Jenekhe, *Macromolecules* 28, 1180 (1995).
21. S.S. Harilal, C.V. Bindhu, V.P.N. Nampoori, and C.P.G. Vallabhan, *J. Appl. Phys.* 86, 1388 (1999).
22. L.W. Tutt and T.F. Boggess, *Prog. Quantum Electron.* 17, 299 (1993).
23. R. Philip, G. Ravindrakumar, N. Sandhyarani, and T. Pradeep, *Phys. Rev. B* 62, 13160 (2000).
24. R.S. Santosh Kumar, S. Venugopal Rao, L. Giribabu, and D. Narayana Rao, *Chem. Phys. Lett.* 447, 274 (2007).
25. I. Cohanoschi, M. Garcia, C. Toro, K.D. Belfield, and F.E. Hernandez, *Chem. Phys. Lett.* 430, 133 (2006).
26. S.S. Nair, J. Thomas, C.S. Suchand Sandeep, M.R. Anantharaman, and R. Philip, *App. Phys. Lett.* 92, 171908 (2008).
27. P. Wang, H. Ming, J. Xie, W. Zhang, X. Gao, Z. Xu, and X. Wei, *Opt. Commun.* 192, 387 (2001).
28. Q. Zheng, S.G. He, C. Lu, and P.N. Prasad, *J. Mater. Chem.* 15, 3488 (2005).
29. T. Cassano, R. Tommasi, M. Tassara, F. Babudri, A. Cardone, G.M. Farinola, and F. Naso, *Chem. Phys.* 272, 111 (2001).